Cancer Imaging (2013) **13(4),** 527–539
DOI: 10.1102/1470-7330.2013.0048

REVIEW

Malignant abdominal rocks: where do they come from?

Joan M. Cheng[a,b], Sree Harsha Tirumani[a,b], Kyung Won Kim[a,b], Sachin S. Saboo[b], Juan C. Baez[b], Atul B. Shinagare[b]

[a]Department of Imaging, Dana Farber Cancer Institute, Harvard Medical School, 450 Brookline Avenue, Boston, MA 02215, USA [b]Department of Radiology, Brigham and Women's Hospital, Harvard Medical School, 75 Francis Street, Boston, MA 02115, USA

Corresponding address: Sree Harsha Tirumani, Department of Imaging, Dana Farber Cancer Institute, Harvard Medical School, 450 Brookline Avenue, Boston, MA 02215, USA.
Email: stirumani@partners.org

Date accepted for publication 24 September 2013

Abstract

For the radiologist, calcifications in an abdominal malignancy raise questions of both diagnostic and prognostic significance. Although certain cancers are well known to calcify, such as colorectal and ovarian, malignant abdominal calcifications actually arise from a wide variety of epithelial, mesenchymal, lymphoid, or germ cell neoplasms. The pathophysiology of calcification in abdominal malignancies is heterogeneous and incompletely understood. Calcifications may present primarily, in untreated tumors, or develop during treatment; the latter can occur in variable clinical settings. A basic understanding of the varied pathogenic etiology can assist the radiologist in assessing disease status. By presenting an assortment of calcified abdominal malignancies on computed tomography in varied clinical settings, we aim not only to inform the differential diagnosis, but also to clarify the prognosis of calcifications in abdominal malignancies.

Keywords: *Malignancy; calcifications; computed tomography; abdomen.*

Introduction

Abdominal calcifications have been of interest to radiologists since they were first visualized in the early years of plain radiography, and are a macroscopic window into the patient's underlying microscopic pathology. Since the advent of computed tomography (CT), our increased ability to detect calcification has magnified the importance of understanding their varied etiology, to better inform our differential diagnosis.

Pathologic mineralization in the abdomen, and elsewhere, can occur as a result of calcification or ossification, although both cannot always be differentiated radiologically[1]. Calcification refers to insoluble calcium phosphate crystal deposition in soft tissue, in contrast to ossification, which refers to formation of mature trabecular bone. Metastatic calcification occurs in the setting of hypercalcemia, most commonly attributable to hyperparathyroidism, often secondary to renal dysfunction. Dystrophic calcification occurs in dead tissues with normal serum calcium levels, and can be associated with a wide variety of non-neoplastic conditions including atherosclerosis, granulomatous infection, inflammation, fat necrosis, and "degenerating tumors"[1]. Benign heterotopic ossification can follow trauma (myositis ossificans traumatica) or can be hereditary (myositis ossificans progressiva/fibrodysplasia ossificans)[2].

In our experience at a tertiary care cancer center, we see calcification in a wide variety of primary and metastatic abdominal malignancies (Table 1). In this review, we aim to describe various malignant neoplastic causes of "calcification in abdomen," including a range of epithelial, mesenchymal, and lymphoid malignancies that calcify in a variety of clinical settings. On imaging, calcification can be seen in treatment-naïve primary or metastatic tumors, or it may develop during or after treatment, in the setting of improving or worsening disease.

Epithelial malignancies

Epithelial cancers are the most common cancers, with breast, prostate, colorectal, and lung carcinomas accounting for approximately half of new cancer diagnoses each

Table 1 **Summary of the cancer types, pathogenesis, and prognostic significance of calcification in malignant abdominopelvic tumors**

		Primary	Pathogenesis of calcification	Prognostic significance
Epithelial	Adenocarcinoma	Colon	Unknown	Longer survival
		Ovarian	Usually psammomatous	Worse survival
		Pancreatic	Psammomatous	Unknown
	Neuroendocrine	Small bowel	Fibrosis	Unknown
		Medullary thyroid	Amyloid deposition	Unknown
Mesenchymal	Bone	Osteosarcoma	Mineralization of osteoid matrix	Increases with increased differentiated tumor burden
		Chondrosarcoma	Mineralization of chondroid matrix	Increases with increased differentiated tumor burden
	Soft tissue	Liposarcoma	Metaplasia Osteosarcomatous or chondrosarcomatous differentiation	Worse prognosis
		GIST, primary	Intratumoral necrosis	Unknown
		GIST, treated	Unknown	Disease response
Lymphoid		NHL, primary	Necrosis	Aggressive subtypes
		HD, primary	Fibrosis/degeneration	Nodular sclerosing subtype
		NHL or HD, treated	Necrosis	Disease response
		Multiple myeloma	Amyloid deposition	Unknown
Germ cell tumor			Mature elements: teeth, bone, cartilage Immature elements: necrosis	Unknown

GIST, gastrointestinal stromal tumor; NHL, non-Hodgkin lymphoma; HD, Hodgkin disease.

year in the United States[3]. Among these, adenocarcinomas are the most common source of calcified abdominal masses; specifically, calcified hepatic metastases are most commonly from colorectal primaries, and calcified peritoneal metastases are most commonly from ovarian primaries[4,5].

Colorectal cancer

Approximately 40% of patients with colorectal cancer have liver metastases, including 11–25% of patients present at initial presentation. Of those, 11–28% demonstrate calcification[6,7]. Classically, the mucinous subtype is most likely to calcify and also carries a worse prognosis[8]. However, Easson et al.[9] found that calcification of liver metastases was correlated with better survival, independent of the degree of differentiation. The pathophysiology of this finding was unclear; on histopathologic review, areas of calcification did not seem to be associated with necrosis or hemorrhage. Easson et al. also noted that some of the noncalcified colorectal metastases to the liver developed calcifications during therapy; however, they could find no association with chemotherapeutic agents or response to therapy[9] (Fig. 1).

Elsewhere in the abdomen, colorectal commonly metastasizes to lymph nodes and the peritoneum. Calcified lymph node metastases from colorectal primary are rare[10]. Calcification within peritoneal carcinomatosis can have a range of appearances, including punctate, curvilinear, amorphous, and coarse, and increasing density of calcification may be associated with disease progression (Figs. 2 and 3). Although uncommon, calcified metastases can also be seen to involve other sites, such as skeletal muscle and the adrenal glands[11,12] (Figs. 4 and 5).

Ovarian cancer

Whereas calcified hepatic metastases are most commonly associated with colorectal primaries, calcified peritoneal carcinomatosis is most commonly associated with epithelial ovarian primaries[4]. Unlike colorectal adenocarcinoma, mucinous ovarian adenocarcinoma calcifies infrequently; the most common presentation is instead a cystic mass. Serous papillary ovarian tumors are the most commonly calcified ovarian neoplasm[13]. Particularly in papillary tumors, the calcifications are predominantly psammomatous, in which a single necrotic cell develops lamellated calcifications, forming a psammoma body[14]. In a series by Burkill et al.[13], 13% of serous tumors demonstrated calcification, compared with 4% of mucinous tumors and 8% of all ovarian tumors. In this series, calcification was correlated with lower histologic grade but worse survival. However, the pathologic basis of this finding is unclear. In patients with papillary serous ovarian adenocarcinoma, the degree of calcification may not aid in assessing treatment response. Increasing density of calcification may be seen in disease progression or treatment response (Figs. 6 and 7), although decreasing density of calcification can also be seen with disease progression (Fig. 8).

Appendiceal cancer

Pseudomyxoma peritonei (PMP) is a nonspecific term for mucinous ascites, which can be localized or diffuse. PMP is most commonly associated with appendiceal

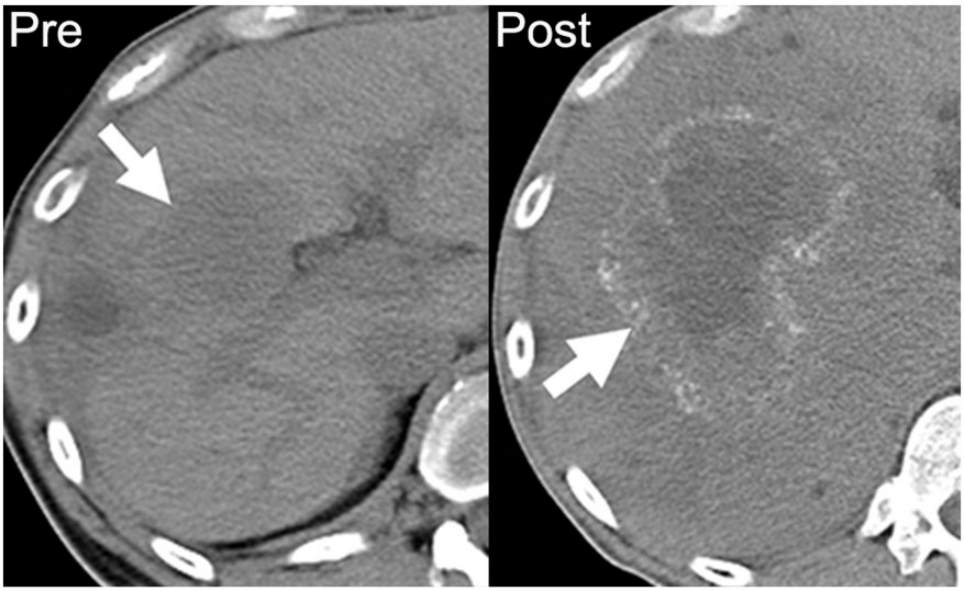

Figure 1 **A 39-year-old man with metastatic mucinous adenocarcinoma of the distal sigmoid colon. Axial noncontrast CT image performed before chemotherapy demonstrates a noncalcified hypodense hepatic metastasis (arrow on left). After 18 months of chemotherapy on multiple regimens, there is an increase in the size of the right hepatic metastasis with a rim of amorphous calcification (arrow on right).**

Figure 2 **A 62-year-old woman with low-grade adenocarcinoma of the sigmoid colon, with focal mucinous features. Axial contrast-enhanced CT shows a curvilinear peritoneal calcification (arrow), which developed following treatment and increased with progressive disease (not shown).**

Figure 3 **A 75-year-old man with moderately differentiated mucinous adenocarcinoma of the colon. Axial contrast-enhanced CT shows a peritoneal implant with coarse peripheral calcification (arrow), which developed while on treatment and increased with progressive disease (not shown).**

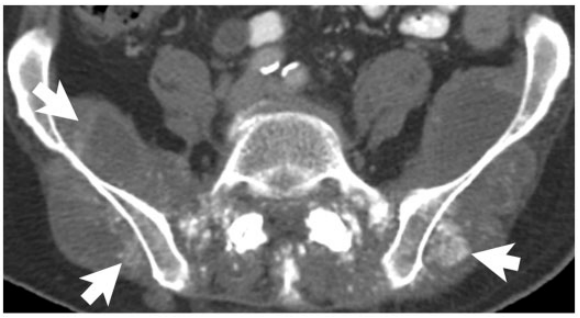

Figure 4 **A 77-year-old man with rectal adenocarcinoma, without mucinous differentiation. Axial noncontrast CT image demonstrates prominent calcification (arrows) in the metastases within the gluteal and paraspinal muscles. These developed while the patient was on chemotherapy.**

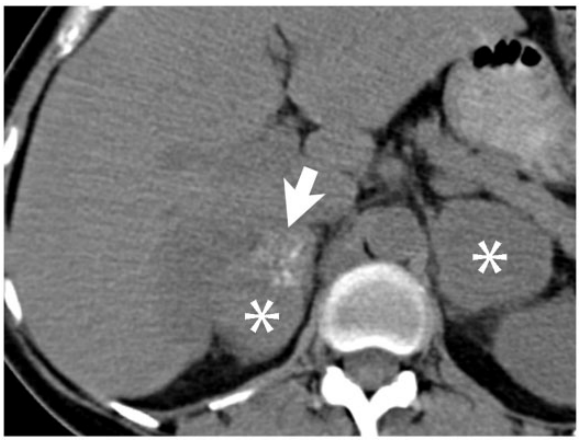

Figure 5 **A 54-year-old woman with adenocarcinoma of the sigmoid colon, without mucinous differentiation. Bilateral adrenal metastases (asterisks) are seen on this axial noncontrast CT image, with amorphous calcification (arrow) within the right adrenal metastasis.**

mucinous adenoma and appendiceal mucinous adenocarcinoma, but can be seen with other primary malignancies such as colorectal, gallbladder, gastric, pancreatic, lung, and breast carcinomas[15]. The distinguishing imaging characteristic of PMP is low-density ascites with serosal implants, which cause scalloping of visceral surfaces. Septations may be seen within the ascitic fluid, representing an interface between the implants or fibrous tissue between them. Dystrophic calcification of these septae or the implants are common, particularly with large-volume disease, and can be helpful in making the diagnosis[16,17] (Fig. 9).

Other epithelial cancers

Although adenocarcinoma is the most common epithelial cancer to calcify, calcification is also possible in other epithelial malignancies. Among pancreatic primaries, calcification is seen in up to 22% of islet cell tumors, but only rarely in ductal adenocarcinoma. Approximately 2% of ductal adenocarcinoma can demonstrate psammomatous calcification[18,19] (Fig. 10). Calcification in pancreatic neuroendocrine tumors may be psammomatous, as in somatostatinomas, or form within amyloid deposits, as in insulinomas[20] (Fig. 11).

Extrapancreatic neuroendocrine tumors can also demonstrate abdominal calcification. Carcinoid tumors, which represent up to 40% of small bowel malignancies, are classically associated with a desmoplastic reaction, tethering small bowel loops and mesenteric calcifications[21]. Up to 60% of small bowel carcinoids are metastatic to the regional lymph nodes or liver at the time of diagnosis. Calcification is seen in up to 70% of metastatic mesenteric nodes[22] (Fig. 12). Medullary thyroid carcinoma is a malignant neuroendocrine tumor arising from the C cells of the thyroid gland, and constitutes less than 10% of cases of thyroid cancer. It is associated with a high incidence of distant metastasis to the lungs, liver, and lymph nodes, which can show dense calcification mimicking granulomatous infection[23] (Fig. 13).

Transitional cell carcinoma (TCC) is the most common malignancy of the urinary tract[24]. TCC can occur anywhere along the urinary tract, but most commonly in the urinary bladder. Calcifications are more common in renal pelvis primaries (seen in 2–7%) than in bladder primaries (<1%)[24]. Superficial calcification is associated with papillary subtypes of TCC, whereas internal calcification is thought to be associated with necrosis[25]. Metastatic spread of TCC is most commonly to lymph nodes, bone, liver, and lung, but a variety of serosal and visceral and soft-tissue sites have also been reported, which can rarely calcify[26] (Fig. 14).

Malignant mesenchymal tumors

Malignant tumors of mesenchymal origin are termed sarcomas, which can be subdivided into soft-tissue sarcomas and bone sarcomas. Excluding gastrointestinal stromal tumors (GISTs), the most common soft-tissue sarcomas are leiomyosarcoma, pleomorphic undifferentiated sarcoma, and liposarcoma[27]. Like adenocarcinomas, soft-tissue sarcomas can develop dystrophic calcifications in areas of cell necrosis or degeneration. A distinctive feature of bone sarcomas is that they can produce osteoid or chondroid matrix, which can mineralize. Soft-tissue sarcomas with osseous or chrondrous metaplasia, or osteoblastic or chondroblastic differentiation, can do the same[28]. Although ossification and calcification are different pathologic processes, their CT appearance is often indistinguishable in extraskeletal masses. Therefore, we include ossified abdominal masses in our discussion of calcified abdominopelvic malignant neoplasms.

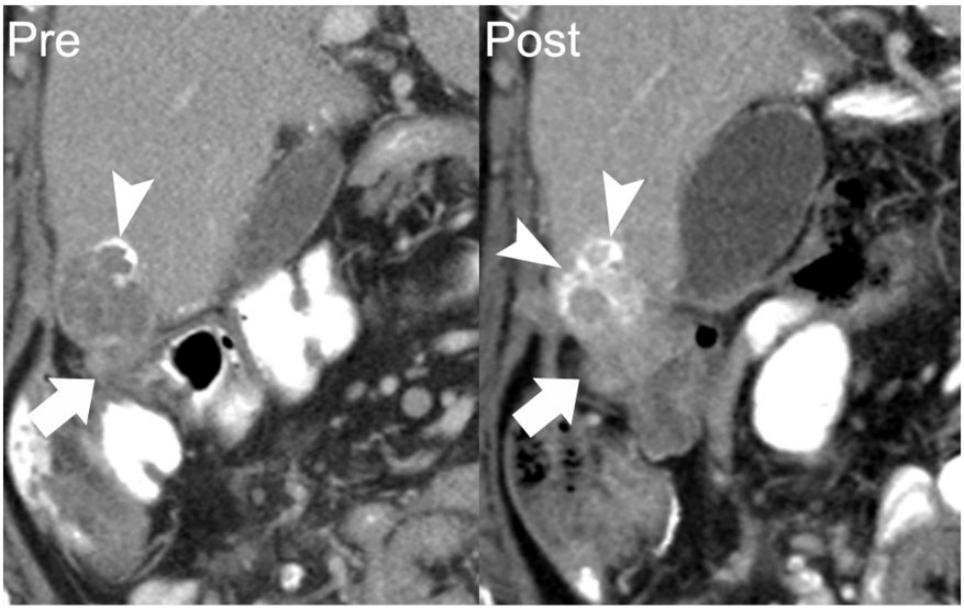

Figure 6 **A 62-year-old woman with papillary serous ovarian adenocarcinoma with calcified peritoneal metastases. Coronal reformatted image from a contrast-enhanced CT shows a perihepatic implant with peripheral calcification (arrow on left). Follow-up CT 11 months later shows the inferomedial component of this lesion to be enlarging (arrow on right). Increasing density of calcification occurred in the setting of disease progression (arrowheads). Over this period, her cancer antigen 125 (CA125) level increased from 57 to 162 units/ml.**

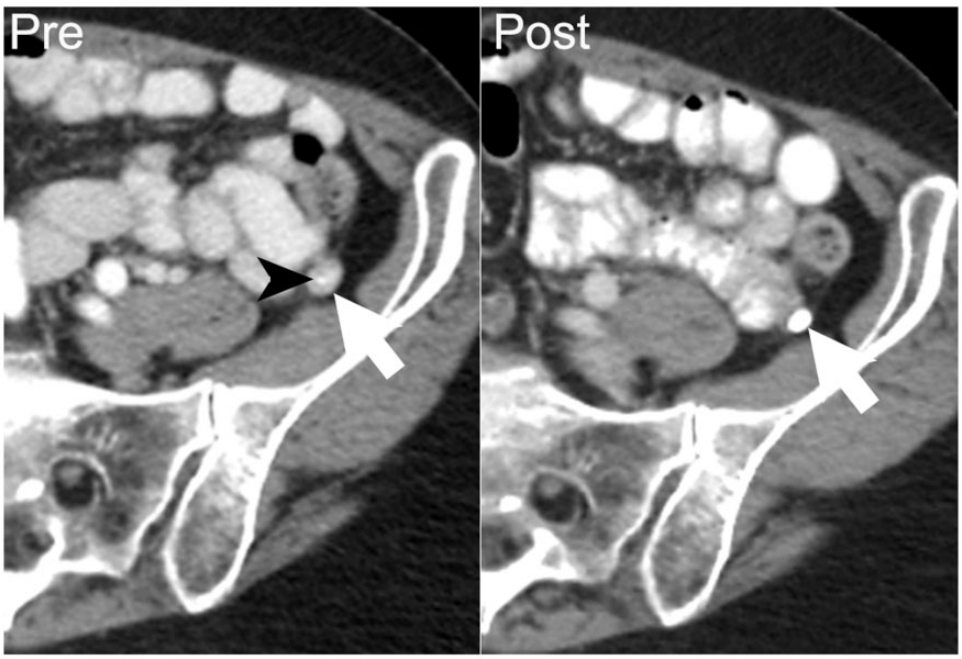

Figure 7 **A 67-year-old woman with papillary serous ovarian adenocarcinoma. Axial contrast-enhanced CT performed at the start of chemotherapy shows an enhancing soft-tissue nodule in left paracolic gutter (arrow on left) with a punctate focus of calcification (arrowhead), compatible with a peritoneal implant. After 8 months of chemotherapy, follow-up contrast-enhanced CT demonstrates increased density of the calcification and decreased size of the left paracolic gutter nodule (arrow on right), indicating that increasing density of calcification may be associated with a treatment response.**

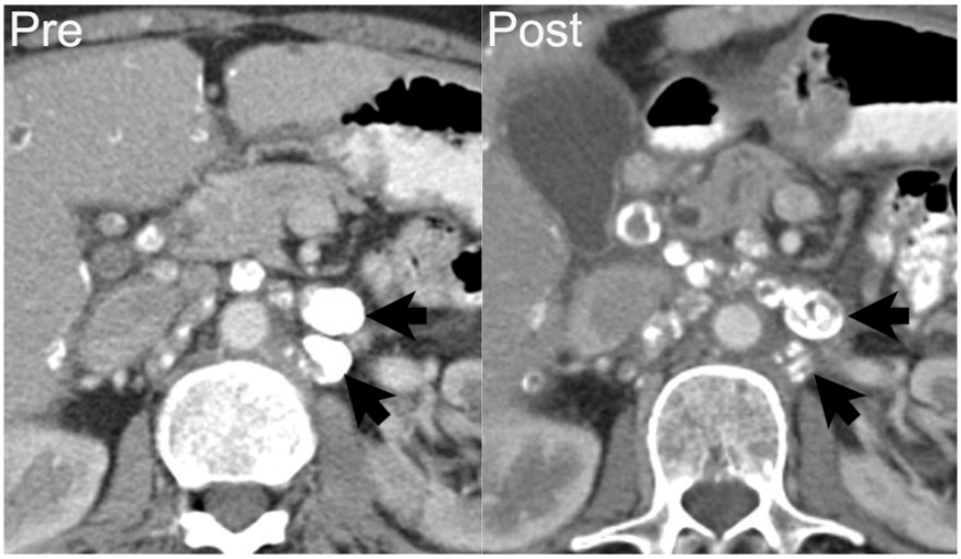

Figure 8 **A 68-year-old woman with endometrioid cystadenocarcinoma of the ovary with metastases to the retroperitoneal lymph nodes. Axial contrast-enhanced CT shows densely calcified left para-aortic lymphadenopathy (arrows on left). After 8 months of chemotherapy, disease progressed with increasing soft tissue and decreasing calcification within the nodes (arrows on right). Over this period, CA125 increased from 1439 to 3838 units/ml.**

Figure 9 **A 45-year-old man with mucinous appendiceal adenocarcinoma. Axial noncontrast CT image demonstrates scalloping (arrowheads) of the liver margin by peritoneal implants and a fine calcified septation (arrow) within the low-density ascites.**

Bone sarcomas

Osteosarcoma is the second most common primary bone sarcoma, with multiple myeloma being the most common primary bone malignancy[29]. By definition, it produces osteoid matrix or immature bone. Cartilaginous elements and chondroid matrix may also be present[29]. Osteosarcoma is an aggressive malignancy that frequently metastasizes by hematogenous dissemination. Up to 30–40% of patients develop metastatic disease despite successful resection and chemotherapy[30]. The most common sites of metastases are the lung and other bones. However, atypical sites of metastases are known to occur, and include brain, epidural space, pleura, pericardium, kidney, liver, adrenal gland, and peritoneal cavity[31]. These atypical sites of metastases are more often found at autopsy, but may be incidentally detected during imaging as calcified masses (Fig. 15). Extraskeletal osteosarcoma is a rare entity accounting for 4% of osteosarcomas, and can be associated with an ossified matrix in 50% of cases. The retroperitoneum is the third most common site of extraskeletal osteosarcoma (8–17% of cases). Similar to skeletal osteosarcoma, extraskeletal osteosarcoma metastasizes to the lung, bone, liver, peritoneum, and brain, and these metastatic deposits can show calcification, irrespective of the mineralization of the primary tumor[32].

Chondrosarcoma is the third most common primary bone malignancy. There are numerous variants, including conventional intramedullary, juxtacortical, and extraskeletal, which have in common cells that produce cartilaginous matrix. The classic “rings and arcs” pattern of mineralization represents endochondral ossification of hyaline cartilage[33]. Intermediate-grade and high-grade chondrosarcomas can metastasize, most frequently to the lung and bones, although the solid abdominal organs and lymph nodes can also be involved[34] (Fig. 16).

Soft-tissue sarcomas

As benign fat necrosis is frequently associated with calcification, calcification of the lipomatous elements of well-differentiated and dedifferentiated liposarcoma can

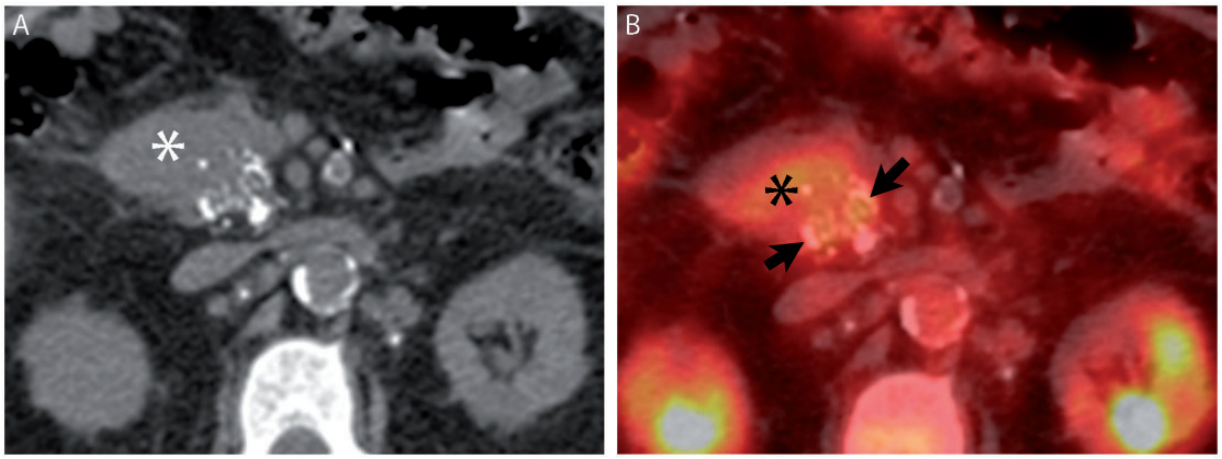

Figure 10 **A 68-year-old man with pancreatic ductal adenocarcinoma. (A) Axial noncontrast CT image from [^{18}F]fluorodeoxyglucose (FDG)-positron emission tomography (PET)/CT demonstrates stippled calcification in a pancreatic head mass (asterisk). (B) Fused image from FDG-PET/CT demonstrates FDG avidity engulfing the calcifications (arrows).**

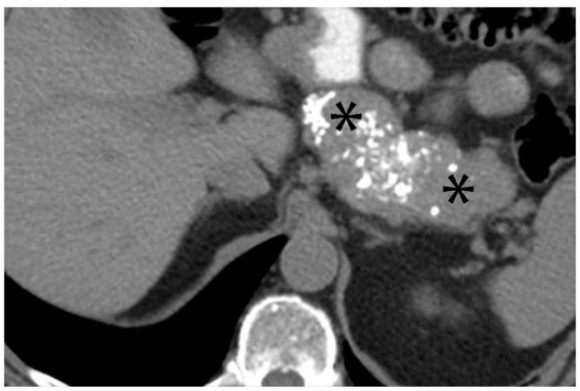

Figure 11 **A 72-year-old man with pancreatic neuroendocrine tumor. Axial nonenhanced CT shows diffusely enlarged pancreatic body and tail (asterisks), with extensive calcification.**

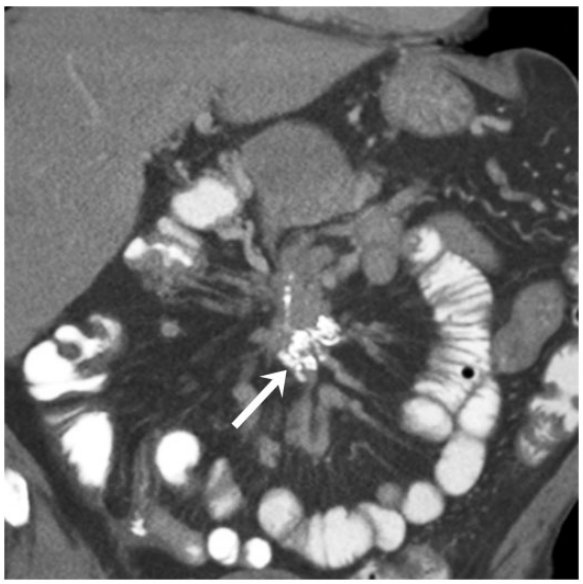

Figure 12 **A 69-year-old man with well-differentiated neuroendocrine carcinoma of the small bowel. Coronal contrast-enhanced CT image demonstrates the typical appearance of this tumor, with a calcified mesenteric mass (arrow) and desmoplastic reaction displacing the small bowel loops peripherally.**

result from fat necrosis[28]. In addition, in a series of 20 patients, Tateishi et al.[35] found calcification or ossification in the soft-tissue components of liposarcoma to be associated with metaplastic elements or osteosarcomatous or chondrosarcomatous differentiation of dedifferentiated liposarcoma. In this series either calcification or ossification in dedifferentiated liposarcoma is associated with a worse prognosis[35] (Fig. 17).

GISTs are the most common form of mesenchymal gastrointestinal neoplasm, but calcification of GISTs is relatively uncommon, with reports in the literature ranging from 3% to 25%[36–38]. Primary calcification is more common in tumors larger than 10 cm, and is generally thought to be dystrophic, associated with intratumoral necrosis (Fig. 18). The tyrosine kinase inhibitors used to treat metastatic GIST induce apoptosis rather than necrosis[39]. Nevertheless, Warakaulle and Gleeson[40] reported in a small series that calcification may occur in the setting of treatment response on tyrosine kinase inhibitor therapy, and our experience has been the same (Fig. 19). The etiology of such calcification in treatment response to tyrosine kinase inhibitors is unclear[39].

Lymphoid malignancies

By definition, lymphoid malignancies originate in lymphoid tissues; these include non-Hodgkin and Hodgkin lymphoma, as well as multiple myeloma. Although they can form solid masses, lymphoma and multiple myeloma originate as "liquid tumors" and, unlike true solid malignancies, they are unresectable regardless of stage. Thus, where appropriate, the radiologist's role is to include them in the differential diagnosis to facilitate the proper clinical management.

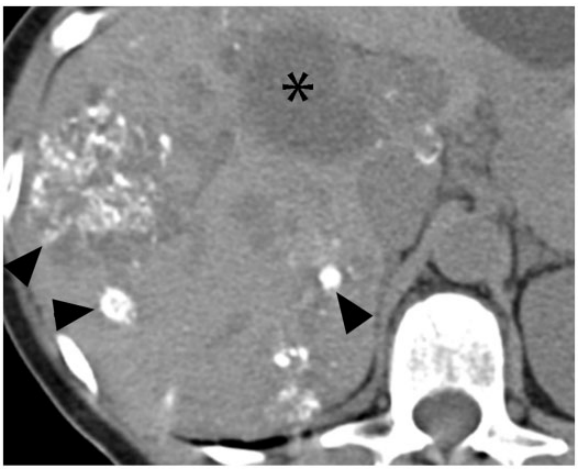

Figure 13 **A 55-year-old woman with medullary thyroid carcinoma. Axial noncontrast CT image demonstrates scattered extensively calcified metastases (arrowheads) and noncalcified metastases (asterisk) in the liver.**

The conventional differential diagnosis for calcified lymphadenopathy or soft-tissue mass in radiology excludes untreated lymphoma[41]. In both Hodgkin and non-Hodgkin lymphoma, calcification in untreated disease is in fact exceedingly rare; in a series of 956 patients, Apter et al.[42] reported calcification in less than 1% of untreated patients. By comparison, in their series 2–8% of lymphoma demonstrated calcification following chemotherapy or radiation therapy. Both primary and treatment-associated calcifications in lymphoma are thought to be dystrophic, associated with cell death or degeneration. Among treated patients, calcification is thought to represent treatment-induced intratumoral necrosis, and is associated with a better prognosis (Fig. 20). In contradistinction, primary calcification and intratumoral necrosis is seen in aggressive forms of non-Hodgkin lymphoma[42]. In Hodgkin lymphoma, both primary and post-treatment calcification is most commonly reported in the nodular sclerosing classical Hodgkin lymphoma. Dystrophic calcification is thought to be associated with the extensive collagen fibrosis and cellular degeneration typical of this subtype[43].

Multiple myeloma is a mature B-cell neoplasm of plasma cells. It is the most common primary bone malignancy, and the extensive osteoclastic bone resorption common in multiple myeloma is associated with hypercalcemia in as many as one-third of patients. This hypercalcemia can lead to diffuse metastatic calcification of soft tissues[44]. Bone scintigraphy is the most sensitive imaging modality for detecting this process, which is often radiographically occult[45]. In addition to metastatic calcification, plasmacytomas of multiple myeloma can demonstrate dystrophic calcification. Like other

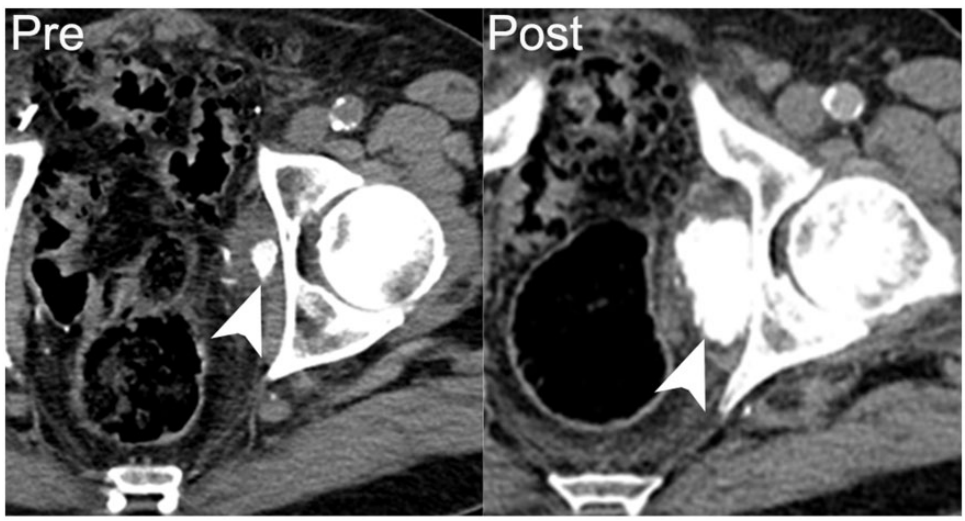

Figure 14 **A 75-year-old man with recurrent papillary transitional cell carcinoma of the bladder. Axial nonenhanced CT image shows a metastasis in the left obturator internus, with dense calcification (arrowhead on left). Following 9 months of chemotherapy the patient's disease progressed, with increasing size and calcification of the left obturator metastasis (arrowhead on right).**

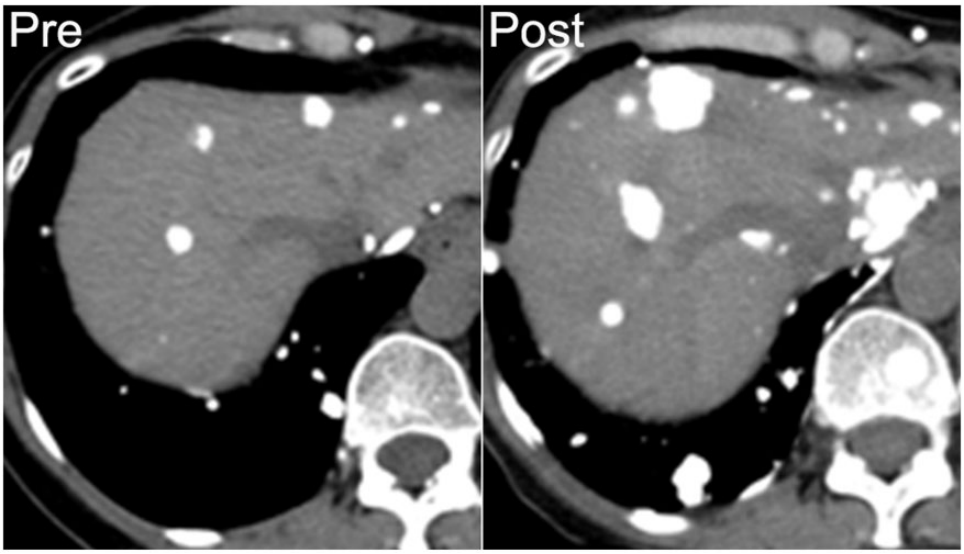

Figure 15 **A 53-year-old woman with metastatic osteosarcoma arising from the sacrum. Mineralized lung and liver metastases are seen on axial noncontrast CT (left). She developed progressive disease after 8 months of chemotherapy, with increasing mineralization in both lung and liver metastases (right).**

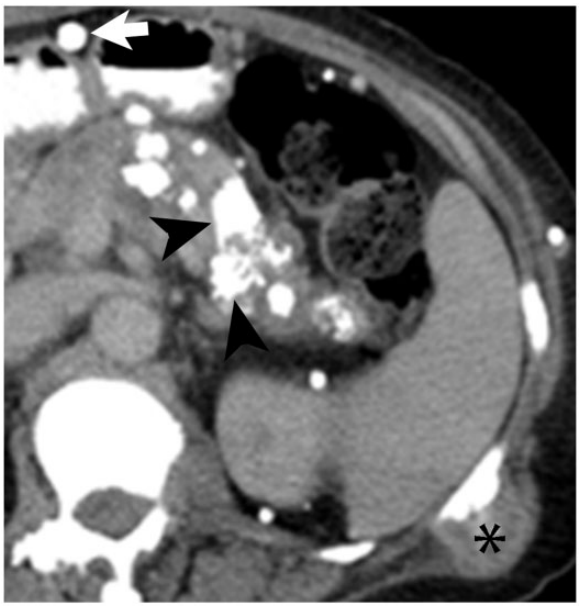

Figure 16 **A 70-year-old woman with extraskeletal mesenchymal chondrosarcoma. Axial contrast-enhanced CT image demonstrates mineralized metastases in the pancreas (arrowheads) and lymph nodes (arrow). Diffuse skeletal metastases involving the vertebrae and ribs are also seen (asterisk).**

Figure 17 **A 62-year-old man with retroperitoneal dedifferentiated liposarcoma. Coronal contrast-enhanced CT image demonstrates a large left lower quadrant mass (asterisk) with coarse internal calcification (arrowhead).**

neoplasms, this can be associated with intratumoral necrosis; unique to myeloma, dystrophic calcifications can also form in areas of amyloid deposition. In a series by Reinus et al.[46], plasmacytomas with calcifications mimicking chondrosarcoma were biopsied, and demonstrated calcification in areas of amyloid deposition (Fig. 21).

Figure 18 **A 50-year-old man with low-risk GIST. Axial noncontrast CT image performed prior to resection shows coarse calcifications in an untreated gastric GIST (arrowheads).**

Malignant germ cell tumors

Germ cell tumors (GCTs) arise from primitive cells that have not yet differentiated into the previously described categories. These most commonly arise in the gonads, with only 1–5% of GCTs arising primarily in extragonadal sites. During embryogenesis, multipotential germ cells migrate along the midline from the yolk endoderm to the gonads. It is believed ectopic germ cells along this path are the source of primary mediastinal GCT and primary retroperitoneal GCT. Primary retroperitoneal GCTs constitute up to 40% of cases of extragonadal GCT[47,48]. Malignant GCTs can be seminomas or nonseminomatous; either can calcify. They are large tumors at presentation and encase, displace, and compress adjacent viscera. Like mature teratomas, in those with mature elements calcifications may arise in mature ectodermal components, such as teeth, or mature mesodermal components, such as bone or cartilage[47,48]. In the absence of mature elements, calcifications are thought to be dystrophic (Fig. 22).

Malignant neurogenic tumors

Neurogenic tumors of the abdomen and pelvis include tumors of the ganglionic system (ganglioneuroma, ganglioneuroblastoma, neuroblastomas), paraganglionic system (pheochromocytoma, paragangliomas) and the nerve sheath (neurofibroma, neurilemmoma, malignant peripheral nerve sheath tumor (MPNST)). Calcification is not uncommon in neurogenic tumors[49]. Ganglioneuromas can demonstrate calcification at the time of presentation in 20% of cases. Coarse amorphous calcification can be seen in up to 55% of cases of

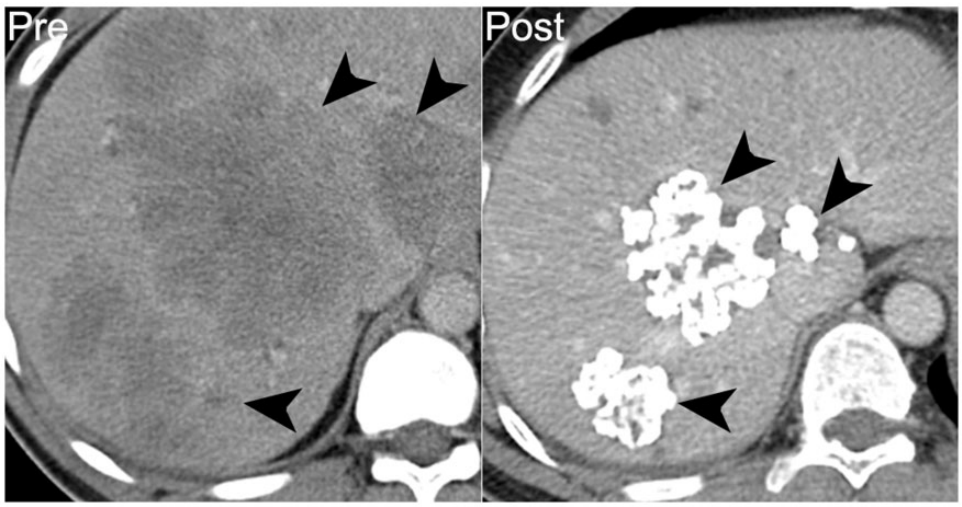

Figure 19 **A 43-year-old man with high-risk jejunal GIST. Prior to treatment, axial noncontrast CT image shows diffuse hypodense hepatic metastases (arrowheads on left). After 6 years of treatment with imatinib mesylate, treated hepatic lesions are smaller and densely calcified (arrowheads on right).**

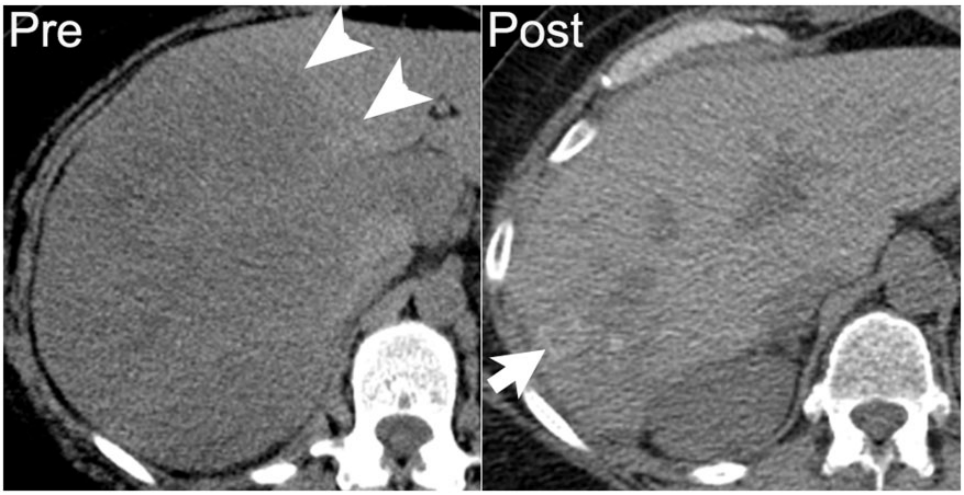

Figure 20 **A 52-year-old woman with diffuse large B-cell lymphoma. Axial noncontrast CT image demonstrates large hypodense mass in the right hepatic lobe, which was proved by biopsy to be lymphoma (arrowheads on left). One year later, following chemotherapy and stem cell transplant, the treated hepatic lesion is smaller with amorphous calcification (arrow on right).**

Figure 21 **A 40-year-old man with multiple myeloma, which had relapsed following stem cell transplant. Axial noncontrast CT image demonstrates a soft-tissue mass in the distal pancreas with peripheral calcification (asterisk). On autopsy, the pancreas was found to be entirely replaced by metastatic multiple myeloma with focal areas of necrosis.**

neuroblastoma on plain radiographs[49]. Calcification can be seen in pheochromocytomas in up to 10% of cases. Nerve sheath tumors, especially MPNST, can also demonstrate calcification.

Our approach to malignant abdominal calcifications

Given the wide assortment of abdominopelvic malignancies that produce calcification, in approaching a case of calcified abdominal metastases with unknown primary, a radiologist should start formulating the differential diagnosis by first familiarizing himself or herself with basic elements of the patient's history: gender, age, oncologic history, comorbidities, and exposures. Once any benign causes of calcification are excluded, location alone can often differentiate epithelial, mesenchymal, lymphoid, and germ cell malignancies (Table 1). Morphology of the mass and calcifications is secondary. For example, gastrointestinal and pancreatobiliary adenocarcinomas commonly metastasize to liver, lymph nodes, and peritoneum; bony involvement is less common[50] (Table 2). In a woman with predominantly peritoneal disease, ovarian carcinoma is most likely[13]. As we have shown, these tumors and calcifications can have varied radiographic appearance.

Soft-tissue sarcomas tend to spare the lymph nodes, and the most common sites of metastases are lung, bone, liver, and brain[51]. Sarcomas of the bone, such as osteosarcoma or chondrosarcoma, most commonly metastasize to regional lymph nodes, lungs, and bone[29,34]. Lymphoma uncommonly presents in extranodal sites without lymph node involvement. Large, homogeneous masses are common, and calcification is very rare in untreated patients[42]. Malignant GCTs present with primary tumors in the gonads or along midline extragonadal sites, ranging from intracranial to mediastinal, retroperitoneal or pelvic[47].

Conclusion

Calcified abdominal masses can occur in a wide variety of malignancies and a variety of clinical settings. Colonic and ovarian adenocarcinomas may be the first malignant

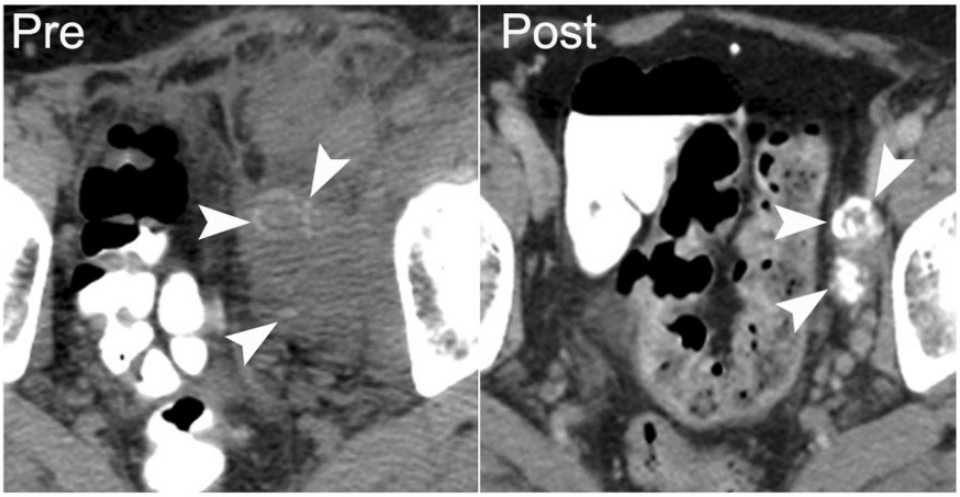

Figure 22 **A 45-year-old man with primary retroperitoneal malignant germ cell tumor. Axial noncontrast CT shows the untreated mass with internal calcification (arrowheads on left), which was confirmed as malignant germ cell tumor with extensive necrosis on core biopsy. Five years after neoadjuvant chemotherapy and partial resection, contrast-enhanced CT shows that the treated tumor is densely calcified with minimal visible soft-tissue component (arrowheads on right).**

Table 2 **Differential diagnoses for calcified malignant abdominopelvic masses**

Calcified malignant abdominopelvic masses	Etiology
Calcified hepatic metastases	Colorectal, pancreatic, ovarian, thyroid cancers, carcinoid tumors, GIST
Calcified peritoneal metastases	Ovarian (serous papillary), colorectal, pseudomyxoma peritonei
Calcified malignant pancreatic tumors	Neuroendocrine tumors, adenocarcinoma
Calcified malignant mesenteric masses	Carcinoid tumor
Calcified malignant renal masses	Renal cell carcinoma, TCC, osteosarcoma metastases
Calcified lymph nodal metastases	Colorectal cancer, carcinoid tumor, treated lymphoma
Calcified malignant retroperitoneal masses	Extraskeletal osteosarcoma, germ cell tumors

GIST, gastrointestinal stromal tumor; TCC, transitional cell carcinoma.

etiology that comes to mind, but a wide range of epithelioid, mesenchymal, lymphoid, and germ cell tumors should be included in the differential diagnosis. Calcifications may be primary or may arise during treatment; the latter are frequently associated with disease progression rather than treatment response. Although much is yet to be understood about the histopathologic basis of calcification of malignant masses, it is clear that calcification in abdominal tumors is not synonymous with necrosis or benignity.

Conflict of interest

The authors have no conflicts of interest to declare.

References

[1] Porth CM. Essentials of pathophysiology: concepts of altered health states. 3rd ed. Philadelphia, PA: Lippincott Williams & Wilkins; 2010.

[2] Subhawong TK, Fishman EK, Swart JE, Carrino JA, Attar S, Fayad LM. Soft-tissue masses and mass like conditions: what does CT add to diagnosis and management? AJR Am J Roentgenol 2010; 194: 1559–1567.

[3] Siegel R, Naishadham D, Jemal A. Cancer statistics, 2013. CA-A Cancer J Clin 2013; 63: 11–30.

[4] Agarwal A, Yeh BM, Breiman BM, Qayyum A, Coakley FV. Peritoneal calcification: causes and distinguishing features on CT. Am J Roentgenol 2004; 182: 441–445.

[5] Scatarige JC, Fishman EK, Saksouk FA, Siegelman SS. Computed tomography of calcified liver masses. J Comput Assisted Tomogr 1983; 7: 83–89.

[6] Stoupis C, Taylor HM, Paley MR, et al. The rocky liver: radiologic-pathologic correlation of calcified hepatic masses. Radiographics 1998; 18: 675–685.

[7] Hale HL, Husband JE, Gossios K, Norman AR, Cunningham D. CT of calcified liver metastases in colorectal carcinoma. Clin Radiol 1998; 53: 735–741.

[8] Ko EY, Ha HK, Kim AY, et al. CT differentiation of mucinous and nonmucinous colorectal carcinoma. Am J Roentgenol 2007; 188: 785–791.

[9] Easson AM, Barron PT, Cripps C, Hill G, Guindi M, Michaud C. Calcification in colorectal hepatic metastases correlates with longer survival. J Surg Oncol 1996; 63: 221–225.

[10] Sweeney DJ, Low VH, Robbins PD, Yu SF. Calcified lymph node metastases in adenocarcinoma of the colon. Australas Radiol 1994; 38: 233–234.
[11] Caskey CI, Fishman EK. Computed tomography of calcified metastases to skeletal muscle from adenocarcinoma of the colon. J Comput Tomogr 1988; 12: 199–202.
[12] Yoshikawa H, Kameyama M, Ueda T, Kudawara I, Nakanishi K. Ossifying intramuscular metastasis from colon cancer: report of a case. Dis Colon Rectum 1999; 42: 1225–1227.
[13] Burkill GJC, Allen SD, A'hern RP, Gore ME, King DM. Significance of tumour calcification in ovarian carcinoma. Br J Radiol 2009; 82: 640–644.
[14] Robbins S, Kumar V, Ramzi S. Robbins and Cotran pathologic basis of disease. 8th ed. Philadelphia, PA: Saunders Elsevier; 2010.
[15] Ronnett BM, Zahn CM, Kurman RJ, Kass ME, Sugarbaker PH, Shmookler BM. Disseminated peritoneal adenomucinosis and peritoneal mucinous carcinomatosis. Am J Surg Pathol 1995; 19: 1390–1408.
[16] Tirumani SH, Fraser-Hill M, Auer R, et al. Mucinous neoplasms of the appendix: a current comprehensive clinico-pathologic and imaging review. Cancer Imaging 2013; 13: 14–25.
[17] Pickhardt PJ, Levy AD, Rohrmann CA, Kende AI. Primary neoplasms of the appendix: radiologic spectrum of disease with pathologic correlation. Radiographics 2003; 23: 645–662.
[18] Ohike N, Sato M, Kawahara M, Ohyama S, Morohoshi T. Ductal adenocarcinoma of the pancreas with psammomatous calcification. Report of a case. JOP 2008; 9: 335–338.
[19] Eelkema EA, Stephens DH, Ward EM, Sheedy PF. CT features of nonfunctioning islet cell carcinoma. Am J Roentgenol 1984; 143: 943–948.
[20] Lewis RB, Lattin GE, Paal E. Pancreatic endocrine tumors: radiologic-clinicopathologic correlation. Radiographics 2010; 30: 1445–1464.
[21] Buckley JA, Fishman EK. CT evaluation of small bowel neoplasms: spectrum of disease. Radiographics 1998; 18: 379–392.
[22] Avcu S, Ozen O, Bulut MD, Bora A. Hepatic metastases of primary jejunal carcinoid tumor: a case report with radiological findings. N Am J Med Sci 2009; 1: 305–308.
[23] Yanardag H, Tetikkurt C, Tetikkurt S. Synchronous lung and liver metastases from medullary thyroid carcinoma. Can Respir J 2003; 10: 39–41.
[24] Wong-You-Cheong JJ, Wagner BJ, Davis CJ. From the archives of the AFIP: transitional cell carcinoma of the urinary tract: radiologic-pathologic correlation. Radiographics 1998; 18: 123–142.
[25] Dinsmore BJ, Pollack HM, Banner MP. Calcified transitional cell carcinoma of the renal pelvis. Radiology 1998; 167: 401–404.
[26] Shinagare AB, Ramaiya NH, Jagannathan JP, Fennessy FM, Taplin M-E, Van den Abbeele AD. Metastatic pattern of bladder cancer: correlation with the characteristics of the primary tumor. Am J Roentgenol 2011; 196: 117–122.
[27] Toro JR, Travis LB, Wu HJ, Zhu K, Fletcher CDM, Devesa SS. Incidence patterns of soft tissue sarcomas, regardless of primary site, in the surveillance, epidemiology and end results program, 1978–2001: an analysis of 26,758 cases. Int J Cancer 2006; 119: 2922–2930.
[28] Toms AP, White LM, Kandel R, Bell RS. Low-grade liposarcoma with osteosarcomatous dedifferentiation: radiological and histological features. Skeletal Radiol 2003; 32: 286–289.
[29] Murphey MD, Robbin MR, McRae GA, Flemming DJ, Temple HT, Kransdorf MJ. The many faces of osteosarcoma. Radiographics 1997; 17: 1205–1231.
[30] Akasbi Y, Arifi S, Lahlaidi K, et al. Renal metastases of a femur osteosarcoma: a case report and a review of the literature. Case Rep Urol 2012; 259193.
[31] Rejin K, Aykan OA, Omer G, et al. Intra-abdominal metastasis in osteosarcoma: survey and literature review. Pediatr Hematol Oncol 2011; 28: 609–615.
[32] Mc Auley G, Jagannathan J, O'Regan K, et al. Extraskeletal osteosarcoma: spectrum of imaging findings. Am J Roentgenol 2012; 198: W31–37.
[33] Murphey MD, Walker EA, Wilson AJ, Kransdorj MJ, Temple HT, Gannon FH. From the archives of the AFIP imaging of primary chondrosarcoma: radiologic-pathologic correlation. Radiographics 2003; 23: 1245–1278.
[34] Ozaki T, Hillmann A, Lindner N. Metastasis of chondrosarcoma. J Cancer Res Clin Oncol 1996; 122: 625–628.
[35] Tateishi U, Hasegawa T, Beppo Y, Satake M, Moriyama N. Primary dedifferentiated liposarcoma of the retroperitoneum. J Comp Assisted Tomogr 2003; 27: 799–804.
[36] Darnell A, Dalmau E, Pericay C, et al. Gastrointestinal stromal tumors. Abdom Imaging 2006; 31: 387–399.
[37] Ghanem N, Altehoefer C, Furtwängler A, et al. Computed tomography in gastrointestinal stromal tumors. Eur Radiol 2003; 13: 1669–1678.
[38] Levy AD, Remotti HE, Thompson WM, Sobin LH, Markku M. From the archives of the AFIP gastrointestinal stromal tumors: radiologic features with pathologic correlation. Radiographics 2003; 23: 283–304.
[39] Izawa N, Sawada T, Abiko R, et al. Gastrointestinal stromal tumor presenting with prominent calcification. World J Gastroenterol 2012; 18: 5645–5648.
[40] Warakaulle DR, Gleeson F. MDCT appearance of gastrointestinal stromal tumors after therapy with imatinib mesylate. Am J Roentgenol 2006; 186: 510–515.
[41] Brant WE, Helms C. Fundamentals of diagnostic radiology. Philadelphia, PA: Lippincott Williams & Wilkins; 2012, p. 1472.
[42] Apter S, Avigdor A, Gayer G, Portnoy O, Zissin R, Hertz M. Calcification in lymphoma occurring before therapy: CT features and clinical correlation. Am J Roentgenol 2002; 178: 935–938.
[43] Panicek DM, Harty MP, Scicutella CJ, Carsky EW. Calcification in untreated mediastinal lymphoma. Radiology 1988; 166: 735–736.
[44] Oyajobi BO. Multiple myeloma/hypercalcemia. Arthritis Res Ther 2007; 9(Suppl 1): S4.
[45] Eagel BA, Stier SA, Wakem C. Non-osseous bone scan abnormalities in multiple myeloma associated with hypercalcemia. Clin Nucl Med 1988; 13: 869–873.
[46] Reinus WR, Kyriakos M, Gilula LA, Brower AC, Merkel K. Plasma cell tumors with calcified amyloid deposition mistaken for chondrosarcoma. Radiology 1993; 189: 505–509.
[47] Shinagare AB, Jagannathan JP, Ramaiya NH, Hall MN, Van den Abbeele AD. Adult extragonadal germ cell tumors. Am J Roentgenol 2010; 195: W274–280.
[48] Rosado-de-Christenson ML, Templeton PA, Moran CA. From the archives of the AFIP. Mediastinal germ cell tumors: radiologic and pathologic correlation. Radiographics 1992; 12: 1013–1030.
[49] Rha SE, Byun JY, Jung SE, Chun HJ, Lee HG, Lee JM. Neurogenic tumors in the abdomen: tumor types and imaging characteristics. Radiographics 2003; 23: 29–43.
[50] DiSibio G, French SW. Metastatic patterns of cancers. Arch Pathol Lab Med 2008; 132: 931–939.
[51] Vezeridis MP, Moore R, Karakousis CP. Metastatic patterns in soft-tissue sarcomas. Arch Surg 1983; 118: 915–918.